SHFM1 deficiency suppresses esophageal squamous cell carcinomas progression via modulating NF-κB signaling and enhancing nature killer cell-mediated tumor surveillance

YIJUAN WU[1,2], ZHIYU WANG[1], SHENGMIAN LI[3], XIANLIANG CHEN[4] and SHENGYUN ZHOU[2]

[1]Department of Oncology and Immunology, The Fourth Hospital of Hebei Medical University, Shijiazhuang, Hebei 050010; [2]Endoscopy Center, Xingtai People's Hospital, Xingtai, Hebei 054031; [3]Department of Gastroenterology, The Fourth Hospital of Hebei Medical University, Shijiazhuang, Hebei 050010; [4]Department of Gastroenterology, Xingtai People's Hospital, Xingtai, Hebei 054031, P.R. China

Received October 27, 2022; Accepted February 28, 2023

DOI: 10.3892/etm.2023.11894

Abstract. Excessive proliferation, metastasis and immune escape are considered to be hallmarks of cancer contributing to tumor progression. Split hand and foot malformation 1 (SHFM1) is highly expressed in various cancers and has been reported to increase malignant behaviors. However, the biological functions of SHFM1 in esophageal squamous cell carcinomas (ESCC) progression remain to be elucidated. An integrated bioinformatics analysis was performed to identify candidate genes in ESCC progression based on GSE microarrays. SHFM1 was found to be profoundly upregulated in ESCC tissues compared with normal tissues and SHFM1 expression was positively associated with poor prognosis. The biological effects of SHFM1 on cell growth, metastasis and immune escape were investigated following depletion or overexpression of SHFM1 *in vitro*. A xenograft mouse model was established to investigate the effect of SHFM1 on ESCC progression *in vivo*. SHFM1 overexpression promoted ESCC cell proliferation and migration *in vitro* as well as tumorigenesis *in vivo*, while SHFM1 knockdown restored those phenotype changes. Additionally, the present study demonstrated that the effects of SHFM1 on malignant behaviors of ESCC cells were achieved by activating the NF-κB signaling accompanied by increased P65 phosphorylation and nuclear translocation. Furthermore, SHFM1 was also found to regulate the sensitivity of cancer cells to natural killer (NK) cells. Specifically, inhibition of SHFM1 enhanced cell-mediated cell apoptosis and increased NK toxicity, which might involve the downregulation of c-Myc and programmed death-ligand 1, key targets in cancer immunotherapy. In conclusion, these findings suggested that SHFM1 probably promoted ESCC progression by activating the NF-κB pathway and enhancing the resistance of ESCC cells to NK cell cytotoxicity, indicating that SHFM1 may be a promising target for ESCC treatment.

Correspondence to: Dr Zhiyu Wang, Department of Oncology and Immunology, The Fourth Hospital of Hebei Medical University, 12 Jiankang Road, Shijiazhuang, Hebei 050010, P.R. China
E-mail: wangzhiyudo2020@163.com

Key words: split hand and foot malformation 1, esophageal squamous cell carcinomas, NF-κB signaling pathway, immune response, malignant behaviors

Introduction

Esophageal cancer (ESCA) is one of the most prevalent malignant cancers worldwide and ranks as the sixth commonest cause of death (1). Esophageal squamous cell carcinomas (ESCC) and adenocarcinoma are two major subtypes of ESCA with broad pathological heterogeneity and together comprise the majority of diagnosed ESCA cases (2). ESCC is the primary histologic type and accounts for >90% of ESCA (3). Currently, the primary clinical therapies have focused on the improvement of patient outcomes, including chemotherapy and surgical resection (4). Extensive tumor cell metastasis remains the primary cause of high mortality and poor prognosis of ESCC (5). Previous reports demonstrate that cancer immunotherapies have been considered a central tool against cancer in the past few decades (6,7). Therefore, it is urgent to elucidate the more specific detection indicators and the underlying pathological mechanism of ESCC.

Split hand and foot malformation 1 (SHFM1) is a key transcription factor that regulates various genes important for embryonic morphogenesis and tumor progression (8). Notably, SHFM1 has been considered an oncogene that is highly expressed in a number of types of human cancer, such as lung cancer, oral squamous cell carcinoma, osteosarcoma and ovarian cancer (9-12). The tumor promotion effect of SHFM1 has attracted great attention. Previous reports indicate that SHFM1 promoted osteosarcoma progression and ablation of SHFM1 inhibited cell proliferation and promoted cell apoptosis both *in vitro* and *in vivo* (10). In addition, SHFM1 exerts tumor promotion effects on ovarian cancer progression and knockdown of SHFM1 causes an inhibition of cell growth and cell cycle progression (12). These emerging findings suggest that SHFM1 expression is closely associated with

tumor progression and considered an oncogene in cancerous development. However, the functional roles of SHFM1 in ESCC progression have yet to be determined. In addition, emerging evidence indicates that SHFM1 is associated with the activation of multiple signaling pathways that participated in tumorigeneses such as the Akt, Notch and Wnt signaling pathways (11,12). It is well established that the NF-κB signaling is aberrantly dysregulated in numerous types of cancer cells and is associated with tumorigenesis (13). However, the role of SHFM1 in the regulation of NF-κB signaling in ESCC progression remains to be elucidated.

The immunotherapy of cancer has been well-documented and the regulation of immune responses serves an important role in tumor progression (14). Notably, natural killer (NK) cell-mediated cellular cytotoxicity is valuable for cancer immunotherapy (15). c-Myc is a proto-oncogene in the majority of types of human cancer (16,17) and promising research indicates that c-Myc expression regulates cytotoxicity-induced apoptosis, which is one of the mechanisms of NK cell-mediated immune response in tumors (18,19). c-Myc acts as a transcriptional target of SHFM1 and SHFM1 overexpression promotes cell proliferation by regulating the transcriptional expression of c-Myc in lung cancer (20). c-Myc could regulate tumor immune response by mediating an immune checkpoint programmed death-ligand 1 (PD-L1) in a number of types of tumors (21-23). Notably, c-Myc can bind to the promoter of PD-L1, thereby positively regulating the expression of PD-L1 in ESCC progression (24). Blockade of PD-L1 by immune checkpoint inhibitors exhibits promising clinical results for antitumor activity via enhancing NK cell responses (25). Hence, the present study hypothesized that SHFM1 also regulated immune response in ESCC progression.

In the present study SHFM1 was identified as a potential biomarker in ESCC through bioinformatics analysis. SHFM1 expression was frequently upregulated in ESCC patient tissues and was significantly associated with clinicopathologic features and overall survival of patients. In addition, the present study focused on the effects of SHFM1 on the malignant phenotypes of ESCC cell lines. Functional studies demonstrated that SHFM1 promoted cell viability, cell cycle progression and migration in ESCC cells and accelerated tumor formation in a xenograft mouse model. Furthermore, the present study specifically assessed whether SHFM1 expression was involved in tumor immunity response in ESCC cells. These findings confirmed the oncogenic role of SHFM1 in the progression of ESCC and highlighted its potential role as a target for ESCC treatment.

Materials and methods

Bioinformatics and database analysis. A total of two gene expression profiles GSE17351 and GSE33810 were selected from the Gene Expression Omnibus (GEO; http://www.ncbi.nlm.nih.gov/geo) database. The GSE17351 dataset included five ESCC and normal tissues. The GSE33810 dataset consisted of one normal and two ESCC samples. The differential expressed genes between ESCC and normal samples were screened by the GEO2R database (http://www.ncbi.nlm.nih.gov/geo/geo2r/). The P-value <0.05 and |log2FC| value >2 were set as significance. The differential genes in ESCC were presented using volcano plots. Venn diagram analysis was performed to explore the overlapped upregulated genes according to these two profiles. Gene Ontology (GO) enrichment and Kyoto Encyclopedia of Genes and Genomes (KEGG) pathways assays were performed using DAVID (https://david.ncifcrf.gov/) to annotate overlapped genes. Protein-protein interaction (PPI) network was constructed to analyze the interactions among selected proteins. Kaplan-Meier plots (http://www.kmplot.com/analysis/index.php?p) database was performed to explore the correlation between gene expression and overall survival. The Gene Set Cancer Analysis database (GSCA; http://bioinfo.life.hust.edu.cn/GSCA) was performed to analyze SHFM1 expression across The Cancer Genome Atlas (TCGA) cancer types. The expression level of SHFM1 in clinical cases was validated using the Gene Expression Profiling Interactive Analysis (GEPIA) (http://gepia.cancer-pku.cn/) database and the UALCAN database (http://ualcan.path.uab.edu). UALCAN dataset was also performed to assess the association between SHFM1 expression and clinical parameters of ESCC.

Human tissue samples. A total of 58 patients with ESCC (male, n=41 and female, n=17; age range, 56-87 years; with a median age of 68 years) were harvested from the Xingtai People's Hospital. All procedures were approved by the Ethics Committee of Xingtai People's Hospital (approval no. 2022-021) and conducted according to the guidelines of the Declaration of Helsinki; all patients provided written informed consent prior to entering the study. ESCC and adjacent non-tumor tissues were collected and stored at -80˚C.

Cell culture and transfection. Human ESCC cell lines TE-1 and KYSE-410 were obtained from Zhong Qiao Xin Zhou Biotechnology (cat. no. ZQ0235) and Procell (cat. no. CL-0586), respectively and were cultured at 37˚C with 5% CO_2 in RPMI-1640 medium (cat. no. 31800; Beijing Solarbio Science & Technology Co., Ltd.) supplemented with 10% fetal bovine serum (FBS). Small interfering RNA (siRNA) sequences were designed and synthesized by General Biology (Anhui) Co., Ltd., comprising two siRNA sequences against SHFM1 (siSHFM1-1 and siSHFM1-2) or nonspecific control siRNA (siControl). In brief, 20 μM siRNAs (3.75 μl) and Lipofectamine® 3000 regent (7.5 μl; cat. no. L3000015; Invitrogen; Thermo Fisher Scientific, Inc.) were added to Opti-MEM (125 μl; cat. no. 31985070, Invitrogen; Thermo Fisher Scientific, Inc.) and incubated for 15 min at room temperature. The sequences used in the present study were as follows: siSHFM1-1, 5'-GAUCAAGAAGAUCAUGAAATT-3'; siSHFM1-2, 5'-AGAUCAAGAAGAUCAUGAATT-3'; and siControl, 5'-UUCUCCGAACGUGUCACGUTT-3'. For SHFM1 overexpression, the coding sequence of SHFM1 was constructed to the pcDNA3.1 vector (cat. no. G109090; Youbao Biology). pcDNA3.1 empty vector (cat. no. V79020; Invitrogen; Thermo Fisher Scientific, Inc.) served as a control. Briefly, SHFM1 expression plasmid or empty vector (4 μg) was complexed with 7.5 μl Lipofectamine® 3000 (cat. no. L3000015; Invitrogen; Thermo Fisher Scientific, Inc.) and then incubated for 15 min at room temperature for transfection into TE-1 and KYSE-410 cells. All experiments were performed 48 h after the transfection.

Western blotting analysis. ESCC tissues and cells were lysed using the RIPA buffer (cat. no. P0013B; Beyotime Institute of Biotechnology) with phenylmethylsulfonyl fluoride (cat. no. ST506; Beyotime Institute of Biotechnology) for the isolation of proteins. A BCA protein assay kit (cat. no. P0009; Beyotime Institute of Biotechnology) was used for protein concentration quantification. Equal amounts of proteins (15-30 μg) were loaded into a 10% SDS-PAGE gel (cat. no. P0015; Beyotime Institute of Biotechnology) and blotted to polyvinylidene fluoride (PVDF) membranes (cat. no. LC2005; Thermo Fisher Scientific, Inc.). Following blocking with bovine albumin (5%; BSA; cat. no. BS043; Biosharp Life Sciences) for 1 h at room temperature, PVDF membranes were immunoblotted with antibody against SHFM1 (1:500; cat. no. 10592-1-AP, Wuhan Sanying Biotechnology), c-Myc (1:500; cat. no. 10828-1-AP; Wuhan Sanying Biotechnology), PD-L1 (1:1,000; cat. no. 28076-1-AP, Wuhan Sanying Biotechnology), phosphorylated (p-)P65 (Ser536; 1:1,000; cat. no. AF2006; Affinity Biosciences), P65 (1:1,000; cat. no. AF5006; Affinity Biosciences), matrix metalloproteinase 9 (MMP9) (1:500; cat. no. 10375-2-AP; Wuhan Sanying Biotechnology), or MMP2 (1:1,000; cat. no. 10373-2-AP; Wuhan Sanying Biotechnology), respectively, overnight at 4˚C, followed by the incubation of horseradish peroxidase (HRP)-conjugated goat anti-rabbit (1:10,000; IgG, cat. no. SA00001-2; Wuhan Sanying Biotechnology) at 37˚C for 40 min. The blots were visualized with an ECL detection reagent (cat. no. E003; Seven Sea biotech, China) and protein expression was normalized to β-actin. The blots were detected using the Gel-Pro-Analyzer (cat. no. WD-9413B; Beijing Liuyi Biotechnology Co., Ltd.).

Reverse transcription-quantitative (RT-q) PCR. Total RNA was isolated from ESCC cells (6-well plates at a density of $1x10^6$ cells per well) with TRIpure solution (cat. no. RP1001; BioTeke Corporation) according to the manufacturer's instructions. The synthesis and quantification of cDNA were performed with the Exicycler 96 SYBR Green PCR system (Bioneer Corporation) according to the manufacturer's instructions. qPCR was conducted using the SYBR Green Master Mix (cat. no. SY1020; Beijing Solarbio Science & Technology Co., Ltd.). The PCR program consisted of: 94˚C for 5 min; 94˚C for 20 sec and 60˚C for 30 sec, for 40 cycles. Gene expression was conducted by the method of $2^{-\Delta\Delta Cq}$ (26) and β-actin was used for normalization. Three biological replicates were analyzed for each experiment.The primer sequences were: SHFM1 forward, 5'-ACCTCGGCTTCCTATGGC-3' and reverse, 5'-CTGGGTTTACGAACTTTCTTTG-3'; c-Myc forward, 5'-ACACCCTTCTCCCTTCG-3' and reverse, 5'-CCGCTCCACATACAGTCC-3'; PD-L1 forward, 5'-AACTACCTCTGGCACATC-3' and reverse, 5'-ATCCATCATTCTCCCTTT-3'; β-actin forward, 5'-GGCACCCAGCACAATGAA-3' and reverse, 5'-TAGAAGCATTTGCGGTGG-3'.

Cell Counting Kit-8 (CCK-8) assay. ESCC cells ($3x10^3$ cells) were seeded onto 96-well plates and cultured in RPMI-1640 medium. Following transfection, cell viability was assessed at 0, 24, 48 and 72 h, respectively. The cells were treated with CCK-8 solution (10 μl; cat. no. KGA317; Nanjing KeyGen Biotech Co., Ltd.) and were cultured for another 2 h. Cell proliferation ability was represented by detecting the absorbance value at 450 nm under a microplate reader (800Ts; BioTek Instruments, Inc.).

Cell cycle assay. Cell cycle analysis was performed using the Cell Cycle Analysis kit (cat. no. KGA512; Nanjing KeyGen Biotech Co., Ltd.) according to the manufacturer's protocol. Briefly, the transfected ESCC cells were collected and fixed in 70% cold ethanol at 4˚C overnight. Subsequently, the fixed cells were washed with 1X phosphate-buffered saline (PBS; pH 7.4; Sangon Biotech Co., Ltd.), followed by incubation with the prepared propidium iodide (PI) staining solution in darkness for 30 min. The DNA content was detected using a flow cytometer (NovoCyte; Agilent Technologies, Inc.). Flow Plus software (version 1.5.6; Agilent Technologies, Inc.) was used to analyze the results. The percentage of cells at the G_1, S and G_2 phases were calculated.

Migration and invasion assays. The effect of SHFM1 on the migratory and invasive capabilities of ESCC cells was performed by Transwell assay. For invasion assay, the Transwell chambers were pre-coated with 40 μl of diluted (1:3) Matrigel (cat. no. 3422; Corning, Inc.) at 37˚C for 2 h. In brief, the transfected TE-1 and KYSE-410 cells ($6x10^3$ cells) were suspended and seeded in 200 μl serum-free medium in the top chamber. RPMI-1640 medium (800 μl) containing 10% FBS was added to the bottom chambers. Following cultivation at 37˚C with 5% CO_2 for 24 h, the cells were washed and fixed with 4% paraformaldehyde for 15 min at 37˚C, followed by staining with 0.4% crystal violet solution (cat. no. 0528; Amresco, LLC) at 37˚C for 5 min. The migrated and invaded cells from five random fields were quantified and captured under an inverted light microscope (IX53; Olympus Corporation).

Immunofluorescence assay. P65 localization was developed by the immunofluorescence assay. The transfected ESCC cells were fixed with 4% paraformaldehyde at 37˚C and reacted with 0.1% Triton X-100 (cat. no. ST795; Beyotime Institute of Biotechnology). Following blocking with 1% BSA for 15 min at 37˚C, cells were incubated with an antibody against P65 (1:200; cat. no. A11201; ABclonal Biotech Co., Ltd.) overnight at 4˚C. Cy3-labeled goat anti-rabbit IgG (1:200; cat. no. A27039; Invitrogen; Thermo Fisher Scientific, Inc.) were used as secondary antibodies. Cells were counterstained with DAPI staining solution (cat. no. D106471-5mg, Aladdin, China) for 5 min at 37˚C and the immunofluorescent images were captured using a fluorescence microscope (BX53; Olympus Corporation).

Cell cytotoxicity assay. For cell cytotoxicity assay, NK-92 cells were obtained from Procell Life Science & Technology Co., Ltd. and grown in a specific medium (cat. no. CM-0530; Procell Life Science & Technology Co., Ltd.) at 37˚C with 5% CO_2. The transfected TE-1 and KYSE-410 cells were stained with 5-6-carboxyfluorescein diacetate succinimidyl ester (CFSE; cat. no. S19285; Shanghai Yuanye Biotechnology Co., Ltd.) for 10 min at 37˚C. Following incubation for 24 h, NK-92 cells were co-incubated with TE-1 or KYSE-410 cells (5:1) for 4 h, respectively. TE-1 and KYSE-410 cells were also incubated separately to detect basal levels. The collected cells

were then stained with PI (100 μg/ml) for 5 min at 4˚C. Cells were then examined by flow cytometry (NovoCyte; Agilent Technologies, Inc.). The specific lysis rate was analyzed by Flow Plus software (version 1.5.6; Agilent Technologies, Inc.) according to the following formula: Specific lysis%=(sample ratio-basal ratio) x100%, where ratio=% CFSE+PI+/% CFSE+ (27).

ELISA assay. To assess granzyme B and perforin expression levels, ESCC cells were harvested following transfection for 48 h. NK-92 cells were co-incubated with ESCC cell at 5:1 radio for a further 12 h at 37˚C. The levels of granzyme B (cat. no. EH0157) and perforin (cat. no. EH1487) from culture media supernatants were detected using the human ELISA kits (Wuhan Fine Biotech Co., Ltd.) according to the manufacturer's instructions.

Animal experiments. A total of 24 BALB/c male nude mice (aged 4-5 weeks; weight 15-16 g) purchased from Changzhou Cavince Laboratory Animal Co., Ltd. were used for the xenograft growth assay. Mice were maintained under standard conditions (temperature, 22±1˚C; 45-55% humidity; 12 h light/dark cycle). The mice were randomly divided into four groups (6 mice in each group): The shControl group, the shSHFM1 group, the Vector group and the SHFM1 group; none of nude mice succumbed during the study. For xenograft models, KYSE-410/vector cells or SHFM1-overexpression KYSE-410 cells ($1x10^6$ cells) were subcutaneously injected into the right flank of mice. In addition, a total of $1x10^6$ cells with SHFM1 knockdown or without gene intervention were injected into mice. Tumor volumes $(LxW^2)/2$ were examined every 4 days. Loss of weight >20% of the body weight of mice and tumor position severely impairing usual body function were applied as humane endpoints. After 28 days, the animals were sacrificed using 30% volume/min CO_2. Tumor tissues were dissected and fixed in 4% paraformaldehyde at room temperature for 24 h for further analysis. Mortality was confirmed by observation of cessation of heartbeat, respiratory arrest and dilated pupils. All animal experiments were approved by the Institutional Animal Care and Use Committee of the Xingtai People's Hospital (approval no. 2022-026) and the ARRIVE Guidelines 2.0 for Reporting Animal Research (28) were followed.

Immunohistochemistry (IHC). For IHC staining analysis, the samples were fixed in 4% paraformaldehyde at room temperature overnight. The sections were embedded in paraffin and sliced into 5 μm sections. Tumor sections were deparaffinized with xylene, followed by rehydration with ethanol. The sections were performed by heat-induced epitope retrieval with antigen retrieval buffer and endogenous peroxidase activity was quenched with 3% H_2O_2 for 15 min. The samples were blocked with 1% BSA at 37˚C for 15 min and incubated with antibodies against SHFM1 (1:100; cat. no. DF3220; Affinity Biosciences) or Ki-67 (1:100; cat. no. AF0198; Affinity Biosciences) overnight at 4˚C. Slides were then cultivated with goat anti-rabbit HRP-conjugated secondary antibody (1:500; cat. no. 31460; Thermo Fisher Scientific, Inc.) for 1 h at 37˚C. The sections were counterstained with DAB solution (cat. no. DAB-1031; Fuzhou Maixin Biotech Co., Ltd.). The images were obtained under a light microscope (BX53; Olympus Corporation).

Statistical analysis. GraphPad Prism 8.0 software (Dotmatics) was used for statistical analysis. Statistical tests for data analysis were calculated with Student's t-test or one-way analysis of variance (ANOVA) with Tukey's multiple comparisons test. The data were expressed as the mean ± standard deviation. $P<0.05$ was considered to indicate a statistically significant difference.

Results

Identification of differentially expressed genes in ESCC and analysis. The present study first screened ESCC-related differential genes in two GSE data sets (GSE17351 and GSE33810). The regulated genes were shown in the volcano plot (Fig. 1A). The Venn diagram showed the overlap of two profiles and 75 upregulated genes were screened (Fig. 1B).

Enriched GO and the KEGG pathway analysis was performed with DAVID. As indicated in Fig. 1C, the GO terms showed that 75 upregulated genes were mainly enriched in the extracellular matrix organization and collagen catabolic process on biological process group; collagen-containing extracellular matrix and collagen trimer on cellular component; metallopeptidase activity and extracellular matrix structural constituent on molecular function. In addition, in the KEGG pathway analysis, 75 upregulated genes were mostly enriched on the IL-17 signaling pathway and transcriptional misregulation in cancer.

PPI network analysis and key genes selection. As shown in Fig. 2A, the PPI network revealed a correlation among these significantly co-expressed genes. A significant module was identified and the most significant three node genes were collagen type I alpha 1 (COL1A1), secreted phosphoprotein 1 (SPP1) and SHFM1 (Fig. 2B). Survival analysis was further performed to evaluate prognostic value of these significant genes. Survival analysis data from TCGA indicated a negative association between SHFM1 expression and overall survival rate of patients ($P<0.05$; Fig. 2C). In addition, there was no significant association between COL1A1 or SPP1 expression and survival rate of patients with ESCC. Among these key genes, SHFM1 was identified as a candidate biomarker based on the prognostic value and SHFM1 expression in different types of cancer was performed across TCGA database. Analysis of data from the GSCA database revealed that SHFM1 expression was highly expressed in various types of cancer, including ESCC (Fig. 2D). Furthermore, the SHFM1 expression pattern focused on ESCC in clinical cases was explored based on the GEPIA and UALCAN databases ($P<0.05$; Fig. 2E and F). Consistently, the expression of SHFM1 was markedly higher in ESCC tissues compared with normal esophageal tissues.

SHFM1 expression and clinical-pathological parameters of patients with ESCC. Given that SHFM1 was related to the prognosis of ESCC, the present study further explored the association between SHFM1 expression and clinical parameters based on TCGA datasets. SHFM1 expression in ESCC patients was increased and positively associated with different clinical features, including nodal metastasis status and pathologic stages in ESCC and was not associated with histological grade (Fig. 3A). The present study revealed that

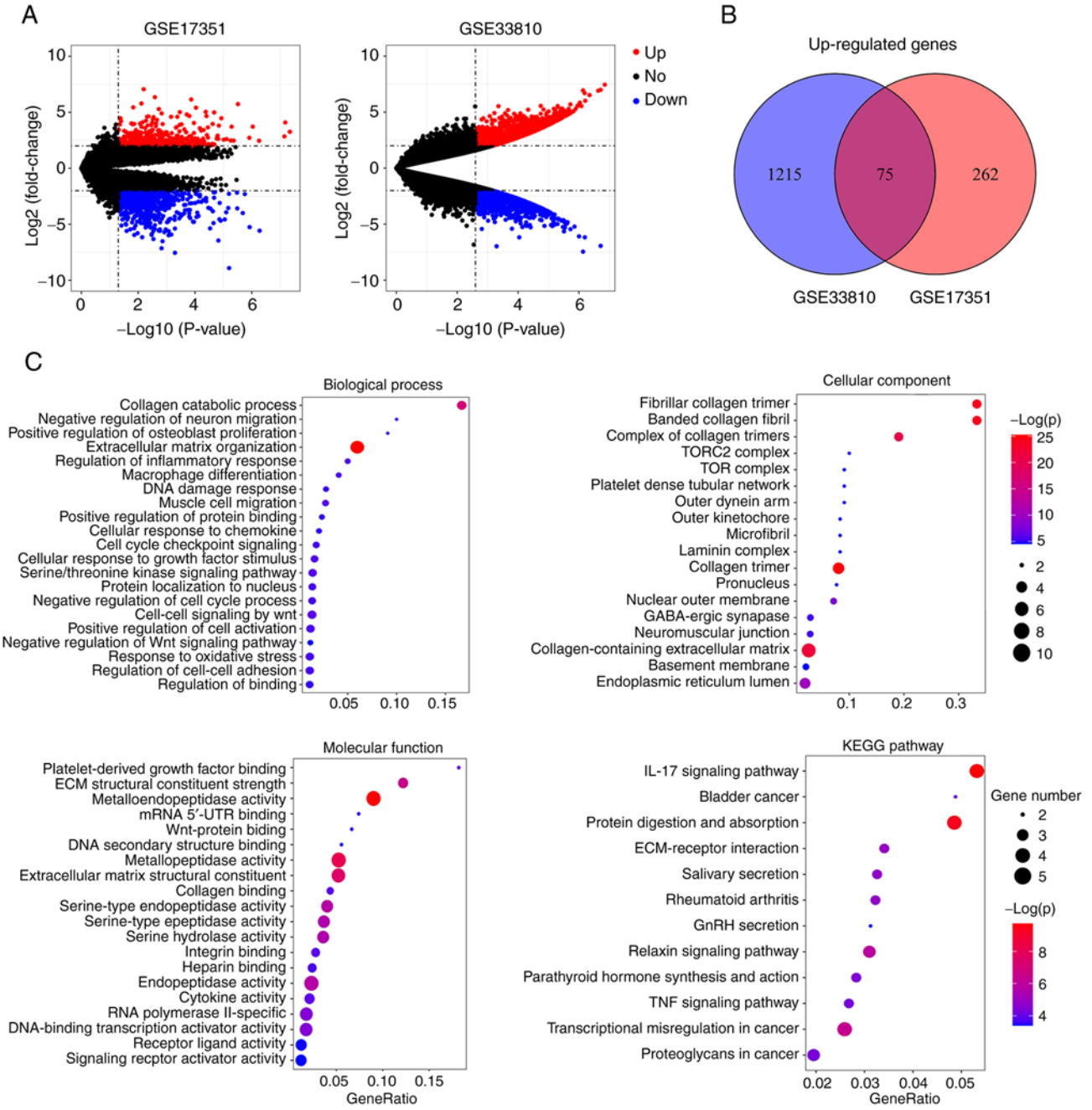

Figure 1. Volcano map and Venn diagram of GSE17351 and GSE33810. (A) volcano map of GSE17351 and GSE33810; red plots for upregulated genes, blue plots for downregulated genes. P<0.05 and log2FC >2 were considered significant. (B) An overlap of 75 upregulated genes was screened on the Venn diagram. (C) The enriched GO terms and KEGG pathway of 75 upregulated genes in ESCC. Bubble diagram of GO enrichment in biological process, molecular function and cellular component. GO, Gene Ontology; KEGG, Kyoto Encyclopedia of Genes and Genomes; ESCC, esophageal squamous cell carcinoma.

SHFM1 expression in the primary tumors with nodal metastasis (N1-N3) was markedly increased compared with those without lymph node metastasis (N0) in ESCC (P<0.01) and SHFM1 expression increased in stages 1-4 compared with normal samples, suggesting that SHFM1 expression was significantly related to the prognosis of patients with ESCC (Fig. 3A). In addition, SHFM1 expression was gradually upregulated with an increase in tumor stages and lymphatic invasion in ESCC. To further confirm the expression of SHFM1 in ESCC progression, 58 ESCC tissues were collected and the correlation among SHFM1 and clinicopathological variables was detected. Notably, SHFM high expression was positively associated with TNM stage (P=0.048) and lymph node metastasis (P=0.006; Table I), this was consistent with database results, suggesting that SHFM might be independent prognostic factor for the patients with ESCC. IHC staining showed that SHFM1 expression was divided into the low expression and high expression groups (Fig. 3B). As shown in Fig. 3C, the protein expression of SHFM1 in ESCC tissues was significantly increased in cancerous tissues compared with adjacent normal tissues.

SHFM1 promotes cell growth and cell cycle progression in ESCC cells. The biological function of SHFM1 in ESCC

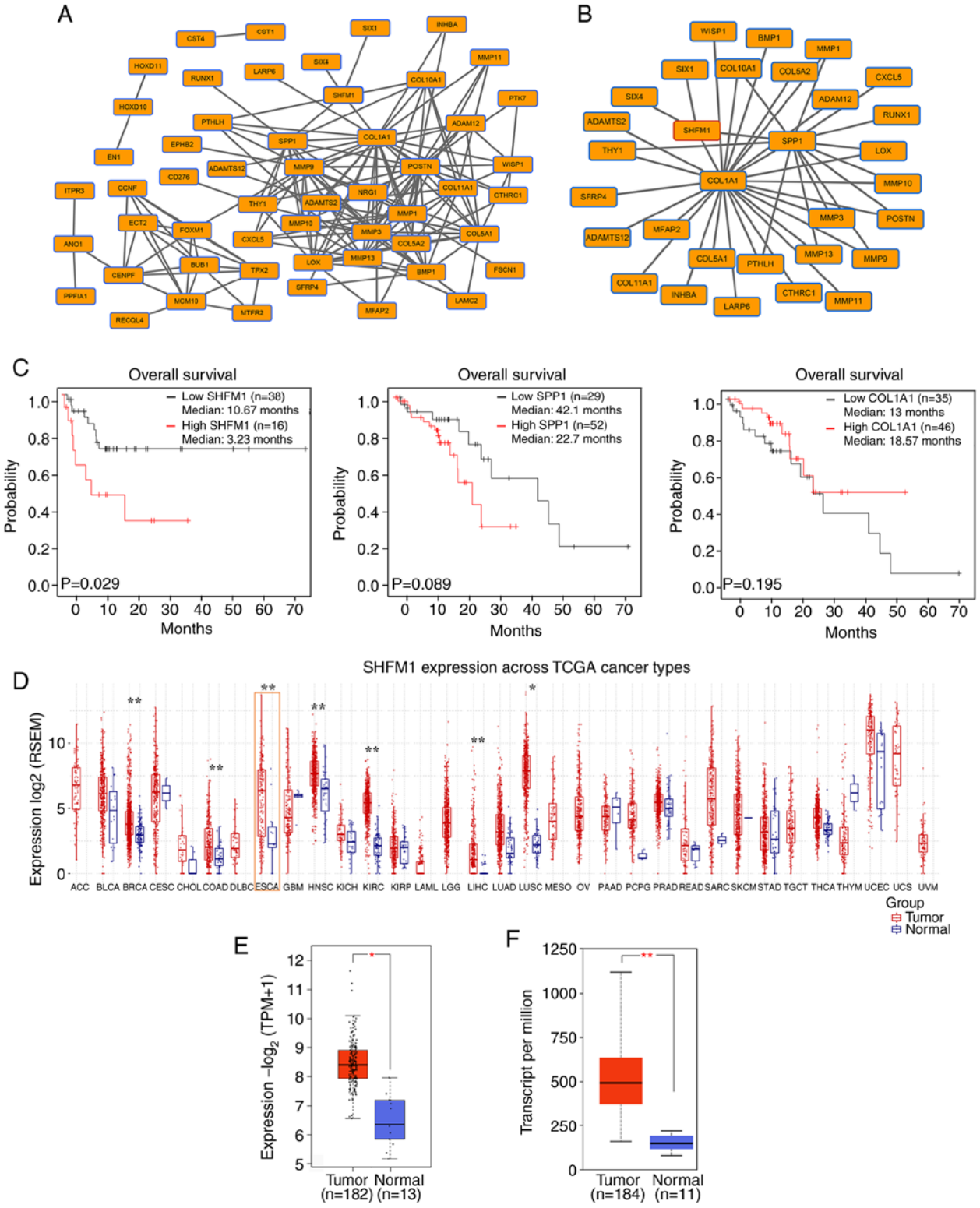

Figure 2. PPI network and gene expression. (A) PPI network of 75 upregulated genes. (B) The significant module was selected from the PPI network. (C) Kaplan-Meier plots analysis of the correlation between selected genes expression and the overall survival. (D) The expression level of SHFM1 in different types of cancer. Red plots represent tumor tissue, blue plots represent normal tissue. (E) SHFM1 was upregulated in patients with ESCC based on the GEPIA database. Red plots represent tumor tissue, blue plots represent normal tissue. (F) SHFM1 expression in patients with ESCC based on the UALCAN database. Red plots represent tumor tissue, blue plots represent normal tissue. Data are presented as the mean ± standard deviation. *P<0.05, **P<0.01 vs. normal group. PPI, protein-protein interaction; SHFM1, split hand and foot malformation 1; ESCC, esophageal squamous cell carcinoma; GEPIA, Gene Expression Profiling Interactive Analysis.

cell lines was further explored. SHFM1 was silenced or overexpressed in ESCC cells by loss-of or gain-of-function approaches. RT-qPCR and western blotting analysis were performed to confirm the expression of SHFM1 following transfection in TE-1 and KYSE-410 cells (Fig. S1A-1D). Subsequently, cell proliferation ability was monitored in ESCC

Table I. Correlation between SHFM1 expression and clinicopathologic parameters in ESCC patients.

Parameters	n	SHFM1 expression		P-value
		High (n=33)	Low (n=25)	
Age (years)				0.114
≥65	40	20 (50%)	20 (50%)	
<65	18	13 (72.2)	5 (27.8%)	
Sex				0.942
Male	41	23 (56.1%)	18 (43.9%)	
Female	17	10 (58.9%)	7 (41.1%)	
TNM stage				0.048*
T1	1	0 (0)	1 (1)	
T2	21	7 (33.3%)	14 (66.7%)	
T3	24	17 (70.8%)	7 (29.2%)	
T4	12	9 (75%)	3 (25%)	
Histological grade				0.359
Low	27	18 (66.7%)	9 (33.3%)	
Middle	22	11 (50%)	11 (50%)	
High	9	4 (44.4%)	5 (55.6%)	
Lymph node metastasis				0.006*
Positive	26	20 (76.9%)	6 (23.1%)	
Negative	32	13 (40.6%)	19 (59.4%)	

SHFM1, split hand and foot malformation 1; ESCC, esophageal squamous cell carcinoma.

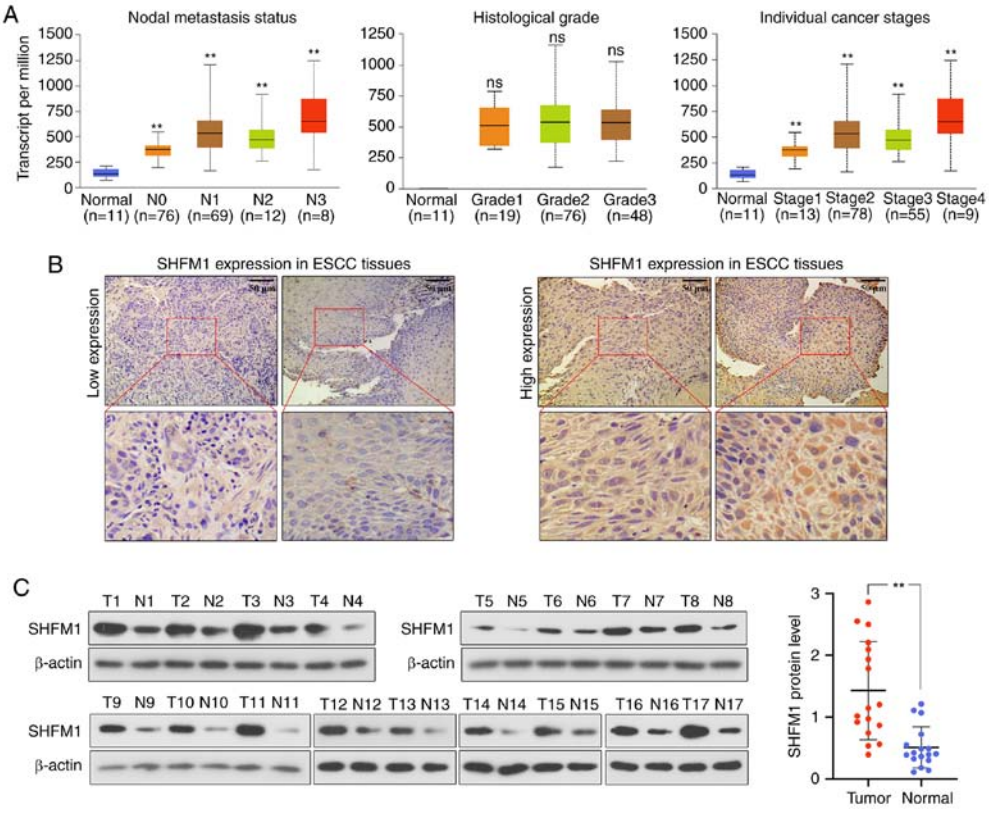

Figure 3. SHFM1 expression based on online database and clinic samples. (A) Expression profile of SHFM1 in patients with ESCC based on different clinical features. (B) The expression of SHFM1 in ESCC tissues was detected by IHC staining. Images were captured at x400 magnification. (C) Expression of SHFM1 in matched 17 ESCC tissues (T) and the non-tumor tissues (N) was explored by western blotting. Relative expression was analyzed and β-actin was used as a normalization control. Data are presented as the mean ± standard deviation. ns, not significant; **P<0.01 vs. normal group. SHFM1, split hand and foot malformation 1; ESCC, esophageal squamous cell carcinoma; IHC, immunohistochemistry.

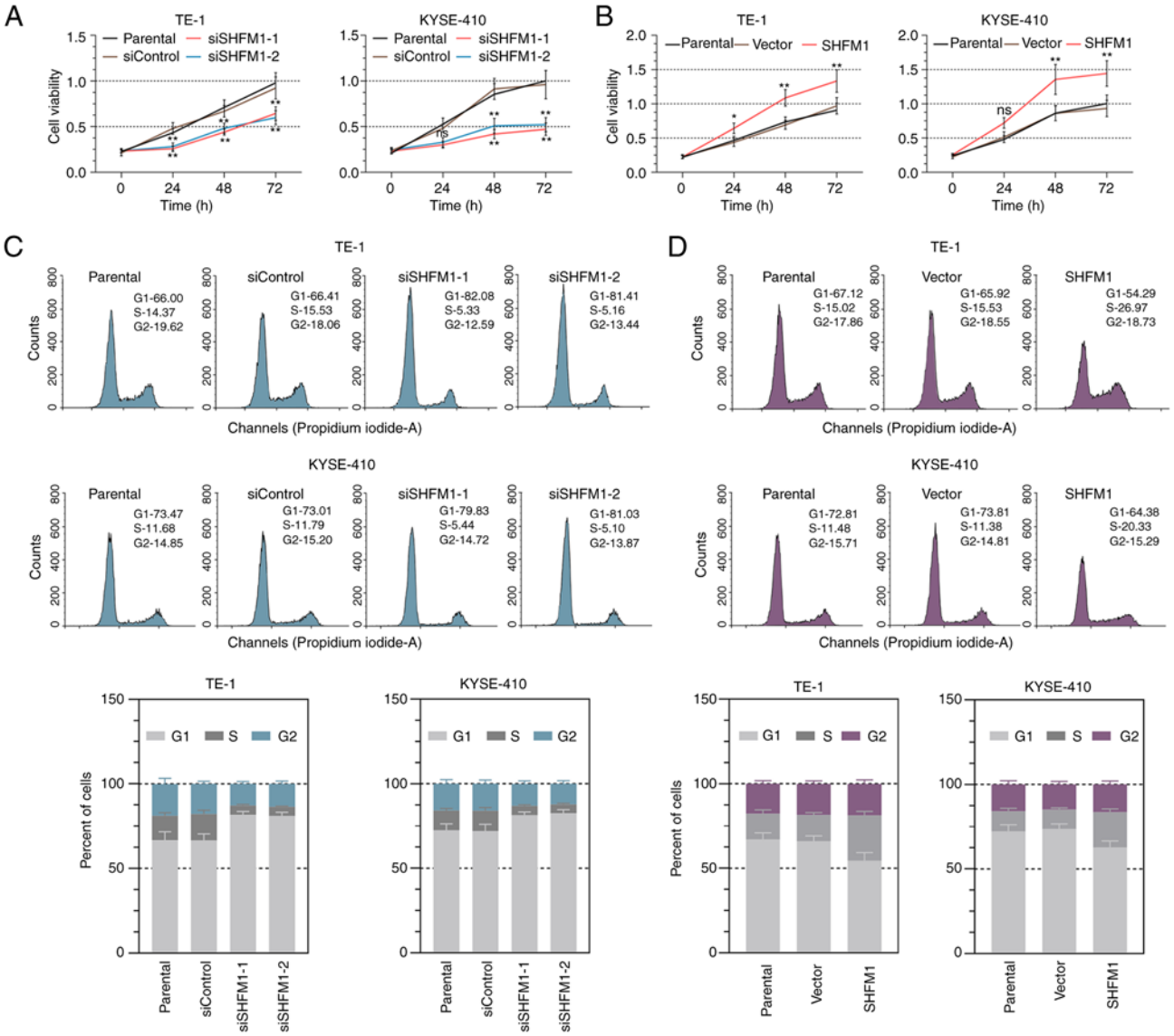

Figure 4. SHFM1 promotes ESCC cell proliferation. (A and B) CCK-8 assays in ESCC cells upon SHFM1 knockdown or overexpression. The images of DNA content were obtained by (C) flow cytometry analysis and (D) quantification of the percentage of cells at the G_1, S and G_2 phases. Data are presented as the mean ± standard deviation. ns, not significant; *P<0.05, **P<0.01, vs. siControl or Vector group. SHFM1, split hand and foot malformation 1; ESCC, esophageal squamous cell carcinoma; si, short interfering.

cells by CCK-8 analysis. The results revealed that knockdown of SHFM1 significantly reduced cell proliferation and the cell viability was increased following SHFM1 overexpression (Fig. 4A and B). To further confirm these results, flow cytometry analysis was conducted to evaluate the role of SHFM1 in cell cycle progression. As shown in Fig. 4C, in the absence of SHFM1, the cell proportion of the G_1 phase was remarkably increased, while the number of cells was decreased in the S phase, suggesting SHFM1 deficiency caused cell cycle arrest in the G_1 phase. by contrast, SHFM1 overexpression caused a decrease in the cell counts of the G_1 phase and was accompanied by increased cells in the S phase (Fig. 4D).

SHFM1 promotes migration and invasion of ESCC cells. Furthermore, the effect of SHFM1 on cell aggressiveness in SHFM1-overexpressed or -silenced cells was determined by Transwell assay. Migration analysis revealed that the downregulation of SHFM1 markedly inhibited the migration capability of TE-1 and KYSE-410 cells and overexpression of SHFM1 markedly increased migration ability and the number of the migrated cells (Fig. 5A and B). In addition, the Matrigel invasion assay indicated that SHFM1 depletion caused a significant decrease in cell invasiveness compared with the corresponding control group and the invasive ability was increased in the SHFM1-overexpressed TE-1 and KYSE-410 cells (Fig. 5C and D).

SHFM1 promotes ESCC tumor growth in vivo. Given that SHFM1 associated with ESCC cell growth *in vitro*, a xenograft tumor model was established to explore whether SHFM1 promoted ESCC progression *in vivo*. As indicated in Fig. 6A and B, the tumors formed by SHFM1-silenced ESCC cells demonstrated a decreased growth rate and reduced tumor volumes compared with those of the control group, while SHFM1 overexpression clearly accelerated ESCC tumor growth *in vivo*. In addition, the contribution of SHFM1 in

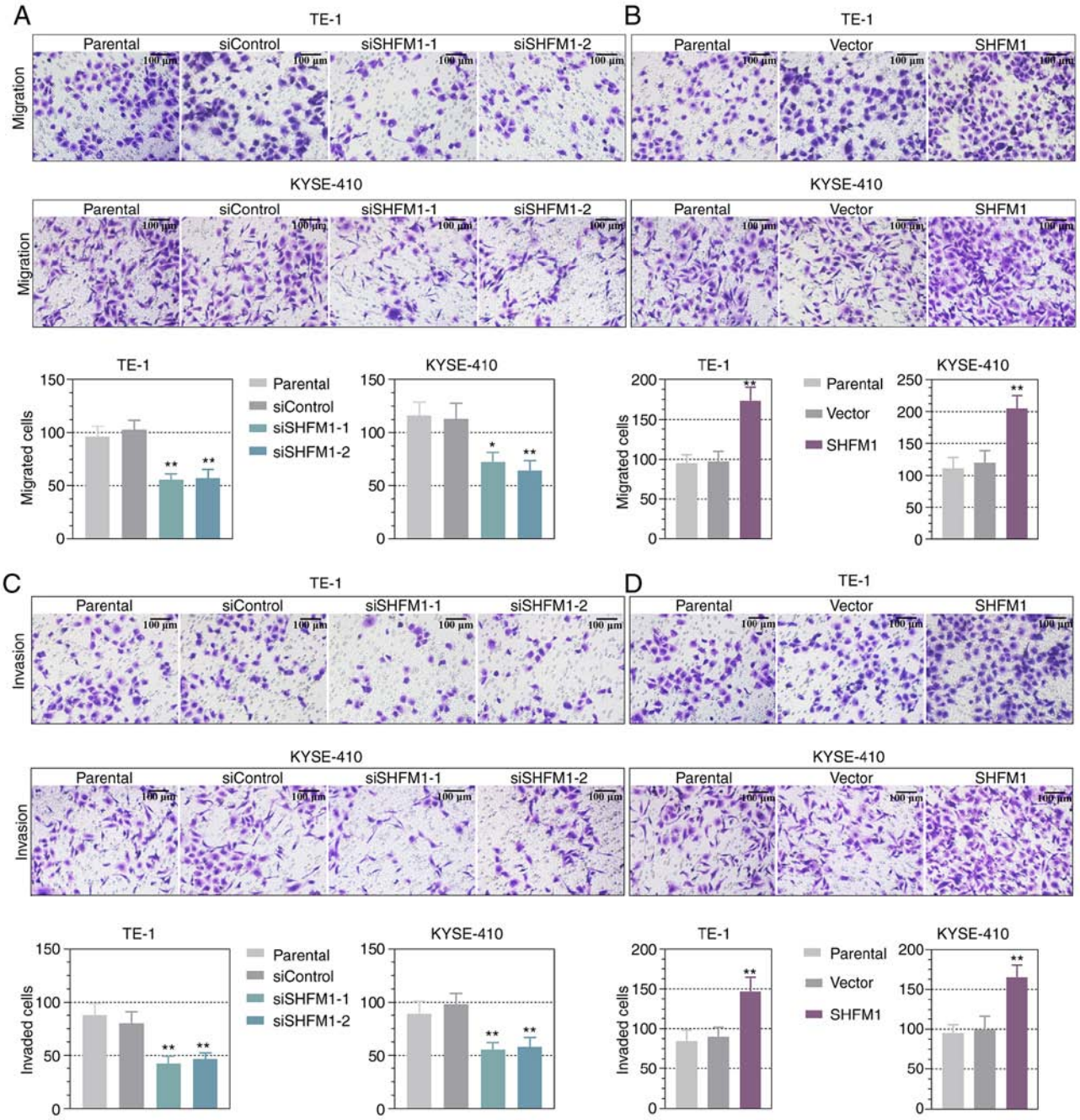

Figure 5. SHFM1 promotes migration and invasion in ESCC cells. The migration and invasion abilities were detected in ESCC cells upon SHFM1 knockdown or overexpression based on Transwell assays; (A) Representative images and (B) quantification of migrated cells. Images were captured at x200 magnification. (C) Representative images and (D) quantification of invaded cells. Images were captured at x200 magnification. Data are presented as the mean ± standard deviation. *P<0.05, **P<0.01 vs. siControl or Vector group. SHFM1, split hand and foot malformation 1; ESCC, esophageal squamous cell carcinoma.

tumor progression *in vivo* was explored. MMP9 and MMP2 expression in ESCC tissues was significantly upregulated in SHFM1-overexpression tumors and downregulated following SHFM1 depletion (Fig. 6C). IHC staining of the xenograft sections demonstrated that overexpression of SHFM1 resulted in increased expression of SHFM1 and Ki-67 levels and SHFM1 and Ki-67 expression was decreased following knockdown of SHFM1 (Fig. 6D and E). These results further suggested that SHFM1 promoted ESCC progression *in vivo*.

Effects of SHFM1 on the NF-κB signaling pathway. The present study further investigated the effect of SHFM1 on the NF-κB signaling pathway. Following transfection for 48 h, ESCC cells were collected to detect the expression of total and phosphorylated P65 content. As indicated in Fig. 7A and B, the knockdown of SHFM1 in ESCC cells markedly decreased the expression levels of phosphorylation of P65, while SHFM1 overexpression strongly promoted P65 phosphorylation and the expression of total P65 protein was not significantly changed. These data suggested that SHFM1 might exert the role in activating the NF-κB signaling pathway. In addition, the location of P65 was further detected by immunofluorescence assay and the results revealed that P65 was located predominantly in the cytoplasm of control cells. Notably, SHFM1 overexpression

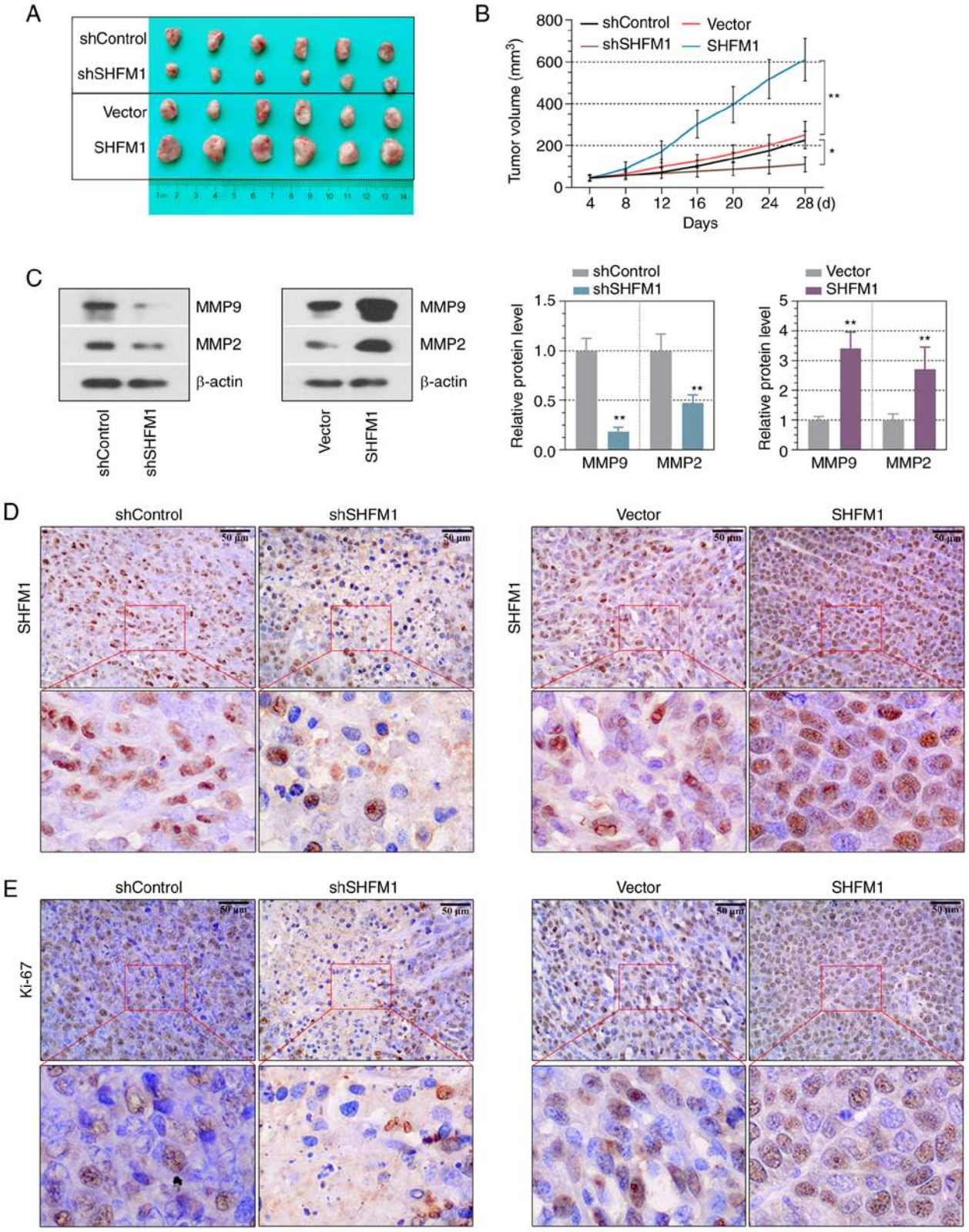

Figure 6. SHFM1 promotes tumor growth *in vivo*. (A) Representative photographs of tumors excised from ESCC tumor-bearing mice. (B) Tumor volume was monitored every 4 days. (C) Western blotting analysis of the expression levels of MMP9 and MMP2 in ESCC tissues. Relative expression was analyzed. (D) SHFM1 and (E) Ki-67 expression in ESCC tissues was detected by IHC staining. Images were captured at x400 magnification. Data are presented as the mean ± standard deviation. *P<0.05, **P<0.01 compared with shControl or Vector group. SHFM1, split hand and foot malformation 1; ESCC, esophageal squamous cell carcinoma; MMP, matrix metalloproteinase; IHC, immunohistochemistry; sh, short hairpin.

showed an increase in nuclear translocation of P65, while P65 was mainly in the cytoplasm of SHFM1-silencing cells (Fig. 7C and D).

Effects of SHFM1 on NK cell-mediated immune response. It is well-known that c-Myc and PD-L1 expression is involved in the immune response in ESCC progression (24,29). Thus,

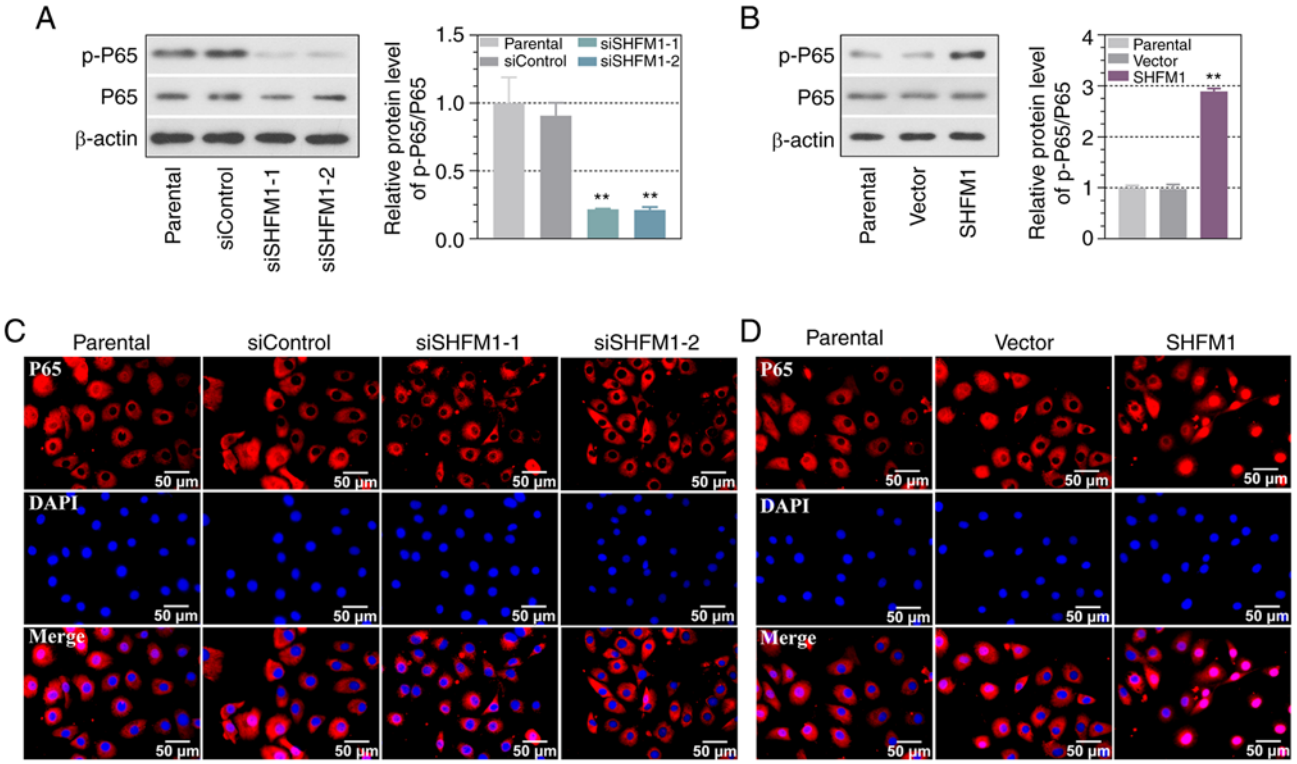

Figure 7. SHFM1 regulates the NF-κB signaling pathway in ESCC cells. (A and B) Western blotting analysis of the expression levels of P65 and p-P65 in the SHFM1 silenced or overexpressed TE-1 cells. The relative expression was analyzed. (C and D) Immunofluorescence analysis indicated the location of P65 in the SHFM1 silenced or overexpressed TE-1 cells. Data are presented as the mean ± standard deviation. **P<0.01 vs. siControl or Vector group. SHFM1, split hand and foot malformation 1; ESCC, esophageal squamous cell carcinoma; si, short interfering; p-, phosphorylated.

the effect of SHFM1 on the expression level of c-Myc and PD-L1 in ESCC cells was investigated. The results revealed that downregulation of SHFM1 significantly reduced c-Myc and PD-L1 levels, while upregulation of SHFM1 enhanced c-Myc and PD-L1 expression in ESCC cells (Fig. 8A-D). It has been reported that human leukocyte antigen (HLA) class-I molecules and PD-L1 on cancer cell surfaces are pivotal for tumor immunity (30). The present study further verified HLA class-I expression in ESCC cells. Results indicated that HLA class-I expression was significantly upregulated following SHFM1 knockdown (Fig. S2). Having shown that SHFM1 knockdown inhibited c-Myc and PD-L1 expression, the present study next explored the effect of SHFM1 on the NK cell-mediated immune cell killing and co-incubated NK cells with ESCC cells. ESCC cells were used as the target cells and NK-92 cells as the effector cells and a CFSE/PI flow cytometry assay was conducted. As shown in Fig. 9A and B, SHFM1 silencing significantly increased the dead target cells, while ESCC cells overexpressing SHFM1 exhibited a decreased number of dead cells, suggesting that knockdown of SHFM1 enhanced the capability of immune cell killing. Additionally, NK-92 cell-mediated specific cell lysis results showed that SHFM1 deficiency increased the percent specific lysis of the ESCC cells, whereas overexpression of SHFM1 yielded the reverse results (Fig. 9C and D). It is generally known that granzyme B and perforin synergize to mediate target cell apoptosis in NK-mediated killing (15,31). The present study detected the expression levels of granzyme B and perforin in culture medium from SHFM1-silenced or -overexpressed ESCC cells that co-cultured with NK-92 cells. The results of ELISA indicated that the knockdown of SHFM1 significantly increased the expression of granzyme B and perforin and upregulation of SHFM1 decreased levels of these cytolytic agents (Fig. 9E-H). These findings suggested that SHFM1 expression partly blocked the susceptibility of cancer cells toward immune attack.

Discussion

In the present study, bioinformatics methods were performed to identify differential genes based on the cohorts profile datasets. GO and KEGG pathway analysis was performed for annotating these genes and PPI network was also developed to identify central node genes. Through bioinformatical analysis, three significant genes were screened, including COL1A1, SPP1 and SHFM1. The clinical significance and function of COL1A1 in ESCC have been well documented in previous studies (32,33). In addition, SPP1 has been identified based on four GEO databases from ESCC samples (34). Thus, SHFM1 was selected as a biological marker in ESCC for further study. Accumulating research indicate that SHFM1 is involved in tumorigenesis in a number of types of human cancer (8,35,36). Consistently, the present study observed a significantly higher level of SHFM1 in ESCC progression based on clinic patient tissues and aberrantly increased SHFM1 expression in cancer patients predicted poor survival. Furthermore, the prognosis value of SHFM1 was investigated based on online databases and clinical cases. It was found that SHFM1 expression was higher in tumors with lymph node metastasis compared with non-metastatic focus. Highly expressed SHFM1 was positively

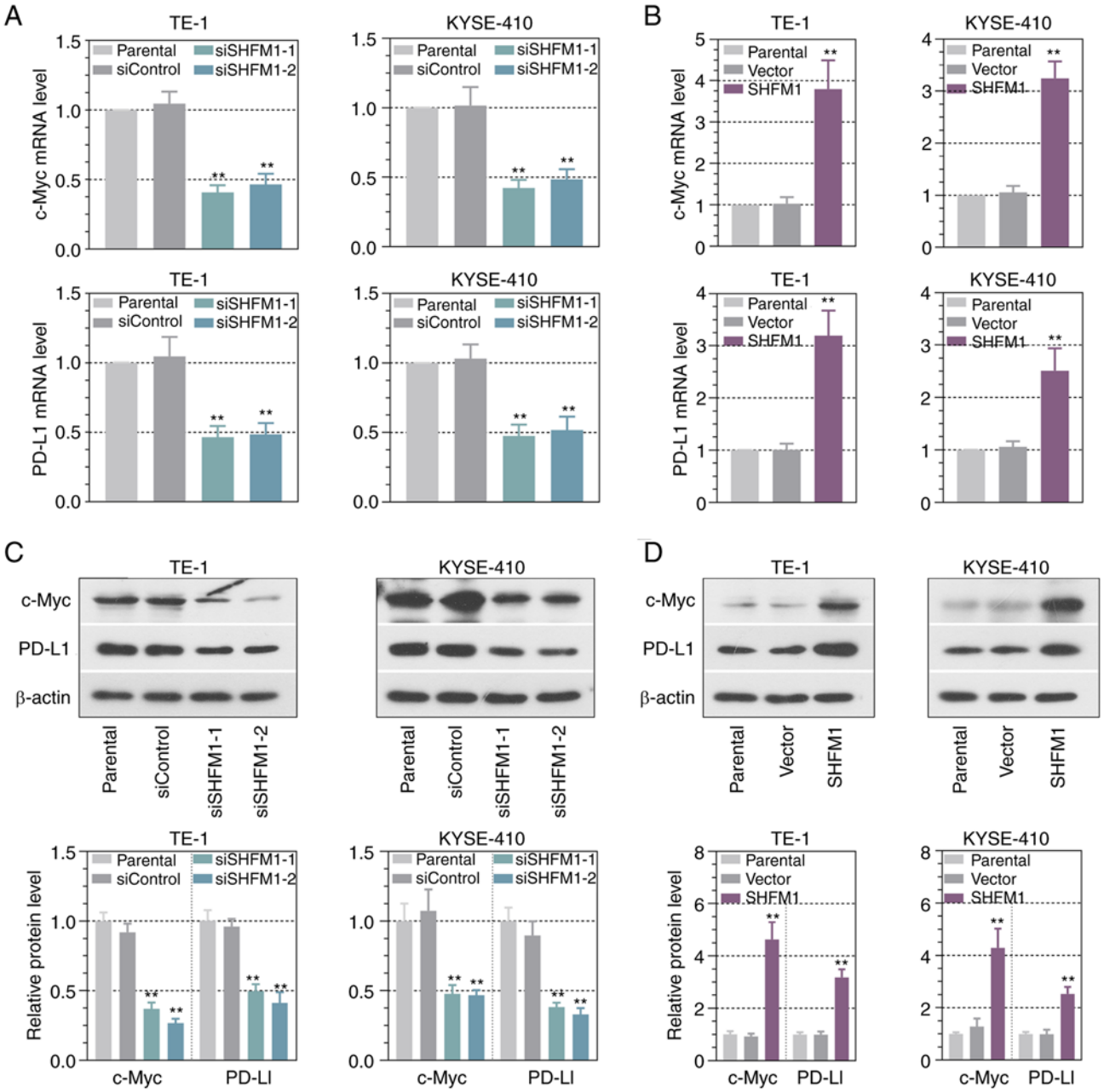

Figure 8. SHFM1 blunts NK cell-mediated cell apoptosis. (A and B) c-Myc and PD-L1 mRNA expression levels were examined by reverse transcription-quantitative PCR in the SHFM1 silenced or overexpressed TE-1 and KYSE-410 cells. (C and D) c-Myc and PD-L1 protein expression levels were examined by western blotting in the SHFM1 silenced or overexpressed TE-1 and KYSE-410 cells. The relative expression was analyzed. Data are presented as the mean ± standard deviation. **P<0.01 vs. siControl or Vector group. SHFM1, split hand and foot malformation 1; NK, natural killer; ESCC, esophageal squamous cell carcinoma; PD-L1, programmed death-ligand 1; PI, propidium iodide; si, short interfering.

associated with lymph node metastasis and TNM stage, indicating a significant association of high SHFM1 expression with tumor growth and metastasis in ESCC. A previous study reported the functional significance of SHFM1 in ESCC progression in that it promotes cell growth, invasiveness ability, colony formation and xenograft growth (37). These findings demonstrated the important role of SHFM1 in cancer progression. Indeed, the present study presented the oncogenic role of SHFM1 in ESCC progression and SHFM1 was associated with the aggressiveness of ESCC cells both *in vitro* and *in vivo*. Suppression of SHFM1 inhibited the proliferation ability and the migrated and invasive capacity of ESCC cells and overexpression of SHFM1 promoted ESCC progression.

Abnormal activation of NF-κB signaling serves a vital role in progressions in various types of cancer, including ESCC (38). It has been indicated that the homeoprotein of SHFM1 is associated with enhanced NF-κB activity in ovarian cancer (39). The present study hypothesized that SHFM1 might exert the functional role in ESCC progression through the regulation of the NF-κB signaling pathway. The data demonstrated that overexpressing SHFM1 increased the expression level of p-P65 and P65 nuclear translocation, suggesting that SHFM1 might regulate the NF-κB pathway by promoting NF-κB nuclear translocation. Furthermore, nuclear translocation of the NF-κB P65 was decreased in SHFM1-silenced ESCC cells. This finding suggested that SHFM1 depletion might be

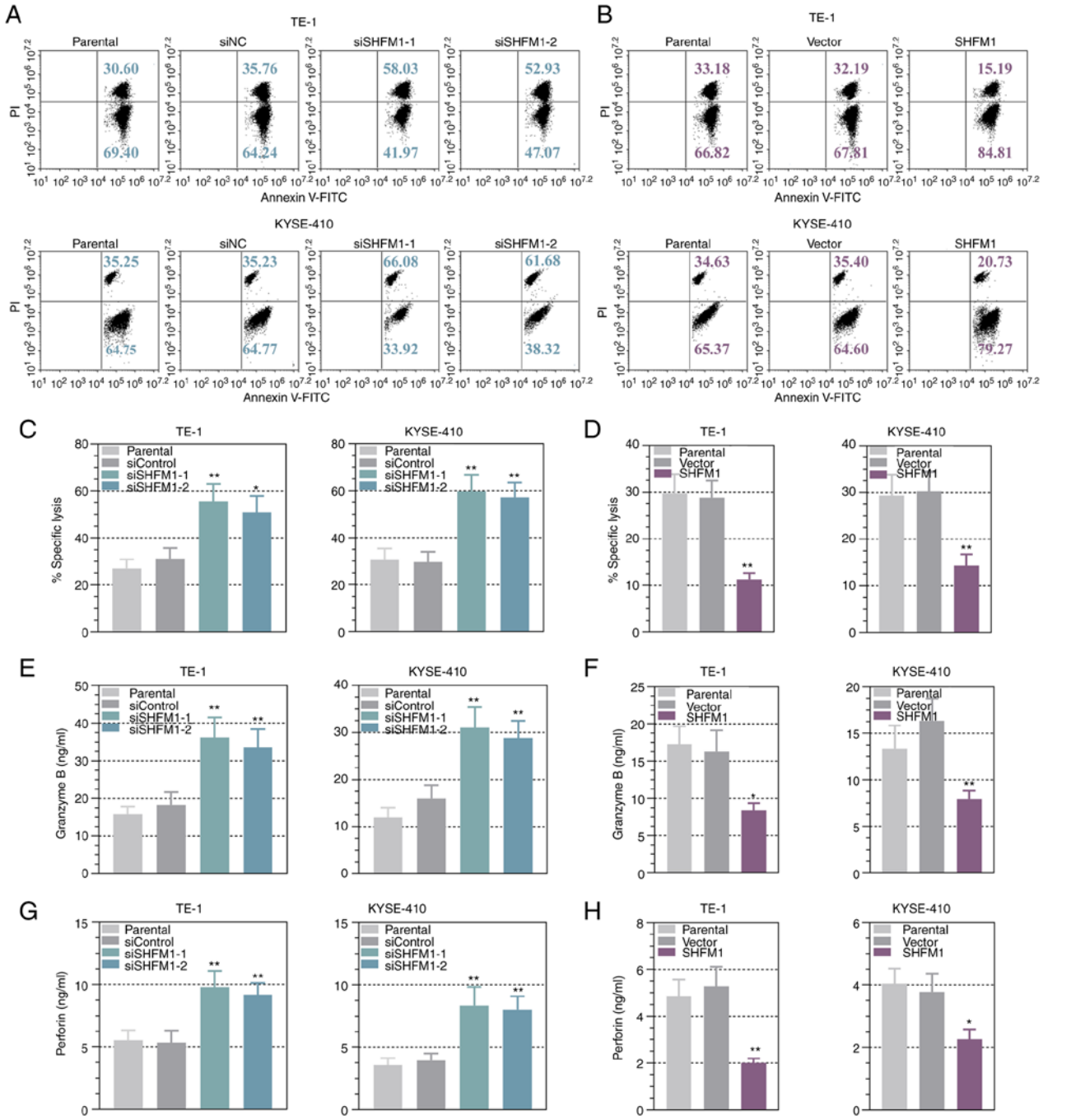

Figure 9. SHFM1 knockdown enhances the ability of immune cell killing. (A and B) Representative images of cell death were obtained by PI staining. (C and D) The specific lysis of ESCC cells was detected using a flow cytometry assay. (E-H) The levels of granzyme B and perforin were observed by ELISA analysis. Data are presented as the mean ± standard deviation. *P<0.05, **P<0.01 vs. siControl or Vector group. SHFM1, split hand and foot malformation 1; ESCC, esophageal squamous cell carcinoma; si, short interfering; NC, negative control.

a valuable approach for the treatment of cancers by regulating the NF-κB signaling pathway in ESCC.

In addition, the present study studied the effect of SHFM1 on the NK cell-mediated immune response in ESCC cells. SHFM1 exerts functional roles through regulating c-Myc expression in lung cancer (11,20). Evidence indicates that the expression of PD-L1 exerts important roles in the malignant progression of various types of human tumors based on the immune response (40,41). PD-L1 is highly expressed in various tumors and elevated PD-L1 expression has been indicated to inhibit the immune response (42). The expression PD-L1 level is commonly regulated by c-Myc in the antitumor immune response (22,43). Thus, the inhibition of PD-L1 and c-Myc could regulate immune responses that benefit tumor immunotherapy (44,45). The present study demonstrated a positive association between SHFM1 expression and c-Myc and PD-L1 levels. SHFM1 knockdown significantly decreased the expression of c-Myc and PD-L1 in ESCC cells. It has been demonstrated that c-Myc and PD-L1 expression is associated with cytotoxicity-induced apoptosis and NK cell responses against tumors (22,46). Therefore, the present study further explored the effect of SHFM1 on cellular cytotoxicity-mediated

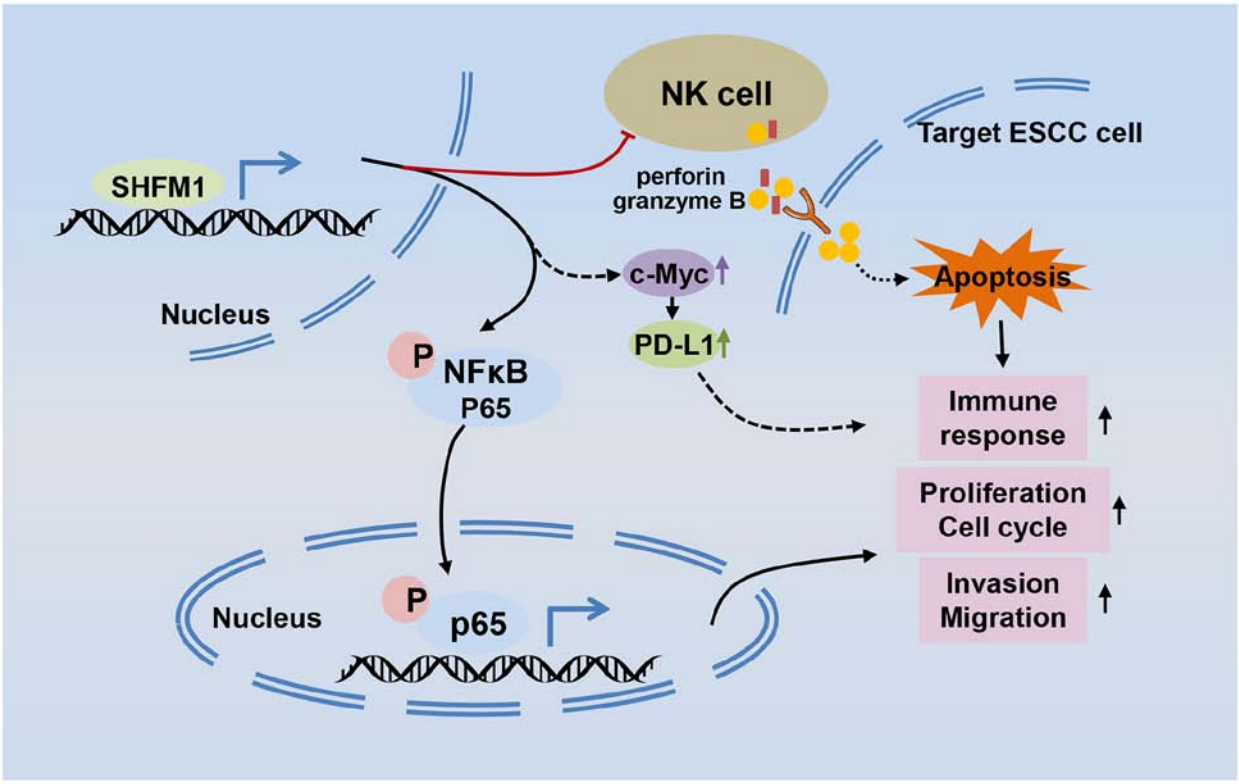

Figure 10. Summary of the results. SHFM1 overexpression promoted esophageal squamous cell carcinomas progression. The mechanism of this action may be associated with the expression of SHFM1 promoting the activation of the NF-κB signaling and blocking nature killer cell-mediated tumor surveillance. SHFM1, split hand and foot malformation 1; ESCC, esophageal squamous cell carcinoma; NK, natural killer; PD-L1, programmed death-ligand 1; p, phosphorylation.

immune response in ESCC. Consistently, immune killing assays were performed to explore the role of SHFM1 in the capacity of cellular cytotoxicity-mediated cell death. Cytotoxic T lymphocytes and NK cells are prevalent players in the innate immune response that exert an antitumor role through recognizing and eradicating cancer cells (47). NK cell-mediated cytotoxicity assay was performed to investigate the cellular and molecular that regulates NK cell anticancer function (48). In the present study, the effect of SHFM1 on NK cell-mediated killing activity was investigated and the percent ESCC cell death was quantified and it was found that suppression of SHFM1 enhanced the ability of immune cell killing of these NK cells on ESCC cells. Notably, ESCC cells overexpressing SHFM1 showed clear resistance to NK cell-mediated cell death. Cellular cytotoxicity is mediated by the secretion of lytic granules, including pore-forming protein perforin and granzymes (15). Perforin-mediated escape of granzymes initiating cell apoptosis is one of the major mechanisms of the ability of NK cells to kill tumor cells (49,50). Thus, the release of perforin and granzymes is vital in cellular cytotoxicity. Inhibition of SHFM1 expression significantly increased the expression levels of perforin and granzyme B. In brief, the increased cell death and lytic granules secretion provided promising evidence of the effect of SHFM1 on immune response during ESCC progression, suggesting that SHFM1 might consider a potential target for ESCC immunotherapy.

The primary mediators of cellular cytotoxicity are CD8+ T cells and NK cells (51). HLA in tumors is another major escape mechanism in cellular cytotoxicity-mediated immune response that is based on triggering tumor specific CD8+ T lymphocyte-mediated responses (52). It has been demonstrated that tumor cells tend to lose expression of HLA class I molecules and reduced expression of HLA class I in tumor cells is associated with mechanisms of tumor escape from immune recognition by tumor-specific cytotoxic T lymphocytes (53) and recovery of HLA class I in cancers is important for T-cell mediated cancer immunotherapy (54). Therefore, HLA class I expression was investigated and it was found that SHFM1 depletion increased HLA class I expression, suggesting that SHFM1 might be involved in T cell-mediated immunity through the regulation of HLA class I. However, information about epigenetic factors for the regulation of HLA-class I expression is limited. The molecular mechanisms underlying SHFM1-dependent HLA-A regulation were not elucidated in the current study. Future work will remedy these deficiencies.

In conclusion, the findings of the current study highlighted the functional role of SHFM1 in ESCC progression. In addition, it further demonstrated that the effects of SHFM1 on the progression of ESCC might be through the regulation of the NF-κB signaling and the effect of SHFM1 on the NK cell-mediated immune response was ascertained (Fig. 10). In summary, the findings of the present study implicated the multi-faceted role of SHFM1 and it might be an attractive diagnostic marker for the therapy of ESCC.

Acknowledgments

Not applicable.

Funding

No funding was received.

Availability of data and materials

The datasets used in the current study are available from the corresponding author on reasonable request.

Authors' contributions

YW and ZW were responsible for the conception and design of the present study. YW and ZW confirm the authenticity of all the raw data. YW, SL and XC obtained the study materials. YW, SL, XC and SZ were responsible for data acquisition and data analysis. YW wrote the manuscript. All authors have read and approved the final manuscript.

Ethics approval and consent to participate

All clinical and animal experiments were approved by the Ethics Committee of Xingtai People's Hospital (approval no. 2022-021). Written informed consent was provided by all patients.

Patient consent for publication

Not applicable.

Competing interests

The authors declare that they have no competing interests.

References

1. Zhou X, Ren T, Zan H, Hua C and Guo X: Novel immune checkpoints in esophageal cancer: From biomarkers to therapeutic targets. Front Immunol 13: 864202, 2022.
2. Jun Y, Tang Z, Luo C, Jiang B, Li X, Tao M, Gu H, Liu L, Zhang Z, Sun S, *et al*: Leukocyte-mediated combined targeted chemo and gene therapy for esophageal cancer. ACS Appl Mater Interfaces 12: 47330-47341, 2020.
3. Abnet CC, Arnold M and Wei WQ: Epidemiology of esophageal squamous cell carcinoma. Gastroenterology 154: 360-373, 2018.
4. Yang YM, Hong P, Xu WW, He QY and Li B: Advances in targeted therapy for esophageal cancer. Signal Transduct Target Ther 5: 229, 2020.
5. Lambert AW, Pattabiraman DR and Weinberg RA: Emerging biological principles of metastasis. Cell 168: 670-691, 2017.
6. He S, Xu J, Liu X and Zhen Y: Advances and challenges in the treatment of esophageal cancer. Acta Pharm Sin B 11: 3379-3392, 2021.
7. Sharma P, Wagner K, Wolchok JD and Allison JP: Novel cancer immunotherapy agents with survival benefit: Recent successes and next steps. Nat Rev Cancer 11: 805-812, 2011.
8. Tan Y and Testa JR: DLX genes: Roles in development and cancer. Cancers 13: 3005, 2021.
9. Zhang J, Wu J, Chen Y and Zhang W: Dlx5 promotes cancer progression through regulation of CCND1 in oral squamous cell carcinoma (OSCC). Biochem Cell Biol 99: 424-434, 2021.
10. Zhang X, Bian H, Wei W, Wang Q, Chen J, Hei R, Chen C, Wu X, Yuan H, Gu J, *et al*: DLX5 promotes osteosarcoma progression via activation of the NOTCH signaling pathway. Am J Cancer Res 11: 3354-3374, 2021.
11. Sun S, Yang F, Zhu Y and Zhang S: KDM4A promotes the growth of non-small cell lung cancer by mediating the expression of Myc via DLX5 through the Wnt/β-catenin signaling pathway. Life Sci 262: 118508, 2020.
12. Tan Y, Cheung M, Pei J, Menges CW, Godwin AK and Testa JR: Upregulation of DLX5 promotes ovarian cancer cell proliferation by enhancing IRS-2-AKT signaling. Cancer Res 70: 9197-9206, 2010.
13. Wang L, Zhou W, Zhong Y, Huo Y, Fan P, Zhan S, Xiao J, Jin X, Gou S, Yin T, *et al*: Overexpression of G protein-coupled receptor GPR87 promotes pancreatic cancer aggressiveness and activates NF-κB signaling pathway. Mol Cancer 16: 61, 2017.
14. Zhang Y and Zhang Z: The history and advances in cancer immunotherapy: Understanding the characteristics of tumor-infiltrating immune cells and their therapeutic implications. Cell Mol Immunol 17: 807-821, 2020.
15. Prager I, Liesche C, van Ooijen H, Urlaub D, Verron Q, Sandström N, Fasbender F, Claus M, Eils R, Beaudouin J, *et al*: NK cells switch from granzyme B to death receptor-mediated cytotoxicity during serial killing. J Exp Med 216: 2113-2127, 2019.
16. Lourenco C, Resetca D, Redel C, Lin P, MacDonald AS, Ciaccio R, Kenney TMG, Wei Y, Andrews DW, Sunnerhagen M, *et al*: MYC protein interactors in gene transcription and cancer. Nat Rev Cancer 21: 579-591, 2021.
17. Wu X, Nelson M, Basu M, Srinivasan P, Lazarski C, Zhang P, Zheng P and Sandler AD: MYC oncogene is associated with suppression of tumor immunity and targeting Myc induces tumor cell immunogenicity for therapeutic whole cell vaccination. J Immunother Cancer 9: e001388, 2021.
18. Zhang P, Wu X, Basu M, Dong C, Zheng P, Liu Y and Sandler AD: MYCN amplification is associated with repressed cellular immunity in neuroblastoma: An in ailico immunological analysis of TARGET satabase. Front Immunol 8: 1473, 2017.
19. Casey SC, Baylot V and Felsher DW: The MYC oncogene is a global regulator of the immune response. Blood 131: 2007-2015, 2018.
20. Xu J and Testa JR: DLX5 (distal-less homeobox 5) promotes tumor cell proliferation by transcriptionally regulating MYC. J Biol Chem 284: 20593-20601, 2009.
21. Casey SC, Baylot V and Felsher DW: MYC: Master regulator of immune privilege. Trends Immunol 38: 298-305, 2017.
22. Casey SC, Tong L, Li Y, Do R, Walz S, Fitzgerald KN, Gouw AM, Baylot V, Gütgemann I, Eilers M and Felsher DW: MYC regulates the antitumor immune response through CD47 and PD-L1. Science 352: 227-231, 2016.
23. Kim EY, Kim A, Kim SK and Chang YS: MYC expression correlates with PD-L1 expression in non-small cell lung cancer. Lung Cancer 110: 63-67, 2017.
24. Liang MQ, Yu FQ and Chen C: C-Myc regulates PD-L1 expression in esophageal squamous cell carcinoma. Am J Transl Res 12: 379-388, 2020.
25. Chiossone L, Vienne M, Kerdiles YM and Vivier E: Natural killer cell immunotherapies against cancer: Checkpoint inhibitors and more. Semin Immunol 31: 55-63, 2017.
26. Livak KJ and Schmittgen TD: Analysis of relative gene expression data using real-time quantitative PCR and the 2(-Delta Delta C(T)) method. Methods 25: 402-408, 2001.
27. Sun X, Zhang J, Hou Z, Han Q, Zhang C and Tian Z: MiR-146a is directly regulated by STAT3 in human hepatocellular carcinoma cells and involved in anti-tumor immune suppression. Cell Cycle 14: 243-252, 2015.
28. Percie N, Hurst V, Ahluwalia A, Alam S, Avey MT, Baker M, Browne WJ, Clark A, Cuthill IC, Dirnagl U, *et al*: The ARRIVE guidelines 2.0: Updated guidelines for reporting animal research. PLoS Biol 18: e3000410, 2020.
29. Lian Y, Niu X, Cai H, Yang X, Ma H, Ma S, Zhang Y and Chen Y: Clinicopathological significance of c-MYC in esophageal squamous cell carcinoma. Tumour Biol 39: 1010428317715804, 2017.
30. Ito S, Okano S, Morita M, Saeki H, Tsutsumi S, Tsukihara H, Nakashima Y, Ando K, Imamura Y, Ohgaki K, *et al*: Expression of PD-L1 and HLA class I in esophageal squamous cell carcinoma: Prognostic factors for patient outcome. Ann Surg Oncol 23: 508-515, 2016.
31. Sefid F, Payandeh Z, Azamirad G, Baradaran B, Afjadi MN, Islami M, Darvish M, Kalantar SM, Kahroba H and Ardakani MA: Atezolizumab and granzyme B as immunotoxin against PD-L1 antigen; an insilico study. In Silico Pharmacol 9: 20, 2021.
32. Li Y, Wang X, Shi L, Xu J and Sun B: Predictions for high and expression resulting in a poor prognosis in esophageal squamous cell carcinoma by bioinformatics analyses. Transl Cancer Res 9: 85-94, 2020.

33. Fang S, Dai Y, Mei Y, Yang M, Hu L, Yang H, Guan X and Li J: Clinical significance and biological role of cancer-derived type I collagen in lung and esophageal cancers. Thorac Cancer 10: 277-288, 2019.
34. Li M, Wang K, Pang Y, Zhang H, Peng H, Shi Q, Zhang Z, Cui X and Li F: Secreted phosphoprotein 1 (SPP1) and fibronectin 1 (FN1) are associated with progression and prognosis of esophageal cancer as identified by integrated expression profiles analysis. Med Sci Monit 26: e920355, 2020.
35. Karsli-Ceppioglu S, Dagdemir A, Judes G, Lebert A, Penault-Llorca F, Bignon YJ and Bernard-Gallon D: The epigenetic landscape of promoter genome-wide analysis in breast cancer. Sci Rep 7: 6597, 2017.
36. Tamilzhalagan S, Muthuswami M, Periasamy J, Lee MH, Rha SY, Tan P and Ganesan K: Upregulated, 7q21-22 amplicon candidate gene SHFM1 confers oncogenic advantage by suppressing p53 function in gastric cancer. Cell Signal 27: 1075-1086, 2015.
37. Huang Y, Yang Q, Zheng Y, Lin L, Xu X, Xu XE, Silva TC, Hazawa M, Peng L, Cao H, *et al*: Activation of bivalent factor DLX5 cooperates with master regulator TP63 to promote squamous cell carcinoma. Nucleic Acids Res 49: 9246-9263, 2021.
38. Zhao Y, Wei L, Shao M, Huang X, Chang J, Zheng J, Chu J, Cui Q, Peng L, Luo Y, *et al*: BRCA1-associated protein increases invasiveness of esophageal squamous cell carcinoma. Gastroenterology 153: 1304-1319.e1305, 2017.
39. Haria D, Trinh BQ, Ko SY, Barengo N, Liu J and Naora H: The homeoprotein DLX4 stimulates NF-κB activation and CD44-mediated tumor-mesothelial cell interactions in ovarian cancer. Am J Pathol 185: 2298-2308, 2015.
40. Chen L and Han X: Anti-PD-1/PD-L1 therapy of human cancer: Past, present, and future. J Clin Invest 125: 3384-3391, 2015.
41. Doi T, Piha-Paul SA, Jalal SI, Saraf S, Lunceford J, Koshiji M and Bennouna J: Safety and antitumor activity of the anti-programmed death-1 antibody pembrolizumab in patients with advanced esophageal carcinoma. J Clin Oncol 36: 61-67, 2018.
42. Wang X, Teng F, Kong L and Yu J: PD-L1 expression in human cancers and its association with clinical outcomes. Onco Targets Ther 9: 5023-5039, 2016.
43. Zhou C, Che G, Zheng X, Qiu J, Xie Z, Cong Y, Pei X, Zhang H, Sun H and Ma H: Expression and clinical significance of PD-L1 and c-Myc in non-small cell lung cancer. J Cancer Res Clin Oncol 145: 2663-2674, 2019.
44. Qu S, Jiao Z, Lu G, Yao B, Wang T, Rong W, Xu J, Fan T, Sun X, Yang R, *et al*: PD-L1 lncRNA splice isoform promotes lung adenocarcinoma progression via enhancing c-Myc activity. Genome Biol 22: 104, 2021.
45. Han H, Jain AD, Truica MI, Izquierdo-Ferrer J, Anker JF, Lysy B, Sagar V, Luan Y, Chalmers ZR, Unno K, *et al*: Small-molecule MYC inhibitors suppress tumor growth and enhance immunotherapy. Cancer Cell 36: 483-497.e415, 2019.
46. Wu Y, Xie J, Jin X, Lenchine RV, Wang X, Fang DM, Nassar ZD, Butler LM, Li J and Proud CG: eEF2K enhances expression of PD-L1 by promoting the translation of its mRNA. Biochem J 477: 4367-4381, 2020.
47. Uppendahl LD, Felices M, Bendzick L, Ryan C, Kodal B, Hinderlie P, Boylan KLM, Skubitz APN, Miller JS and Geller MA: Cytokine-induced memory-like natural killer cells have enhanced function, proliferation, and in vivo expansion against ovarian cancer cells. Gynecol Oncol 153: 149-157, 2019.
48. Lorenzo-Herrero S, Sordo-Bahamonde C, González S and López-Soto A: A flow cytometric NK cell-mediated cytotoxicity assay to evaluate anticancer immune responses in vitro. Methods Mol Biol 1884: 131-139, 2019.
49. Prager I and Watzl C: Mechanisms of natural killer cell-mediated cellular cytotoxicity. J Leukoc Biol 105: 1319-1329, 2019.
50. Zhou Z, He H, Wang K, Shi X, Wang Y, Su Y, Wang Y, Li D, Liu W, Zhang Y, *et al*: Granzyme A from cytotoxic lymphocytes cleaves GSDMB to trigger pyroptosis in target cells. Science 368: eaaz7548, 2020.
51. Cerwenka A and Lanier LL: Natural killer cell memory in infection, inflammation and cancer. Nat Rev Immunol 16: 112-123, 2016.
52. Aptsiauri N, Ruiz-Cabello F and Garrido F: The transition from HLA-I positive to HLA-I negative primary tumors: The road to escape from T-cell responses. Curr Opin Immunol 51: 123-132, 2018.
53. Ramia E, Chiaravalli AM, Eddine FBN, Tedeschi A, Sessa F, Accolla RS and Forlani G: CIITA-related block of HLA class II expression, upregulation of HLA class I, and heterogeneous expression of immune checkpoints in hepatocarcinomas: Implications for new therapeutic approaches. Oncoimmunology 8: 1548243, 2019.
54. Garrido F, Aptsiauri N, Doorduijn EM, Lora AM and van Hall T: The urgent need to recover MHC class I in cancers for effective immunotherapy. Curr Opin Immunol 39: 44-51, 2016.